Schemes to compute unsteady flashing flows

Michel Barret, Eric Faucher, Jean-Marc Hérard

SCHEMES TO COMPUTE UNSTEADY FLASHING FLOWS

Michel Barret[2], Eric Faucher[1,2], Jean-Marc Hérard [3,4]

1 EDF-Division Recherche Développement.
Département MTC
Centre des Renardières. 77250 Moret-Sur-Loing. France

2 Laboratoire Thermique et Mécanique des Fluides.
IUT Sénart. Avenue Pierre Point. 77127. Lieusaint. France
Email adress : barret@univ-paris12.fr

3 EDF- Division Recherche Développement.
Département MFTT.
6,quai Watier. 78400. Chatou. France
Email adress : Jean-Marc.Herard@der.edf.fr

4 Centre de Mathématique et d'Informatique
- LATP - UMR CNRS 6632
Université de Provence. 39, rue Joliot Curie. 13453 Marseille. France
Email adress : Herard@cmi.univ-mrs.fr

Abstract : We provide herein some ways to compute flashing flows in variable cross section ducts, focusing on the Homogeneous Relaxation Model. The basic numerical method relies on a splitting technique which is consistent with the overall entropy inequality. The cross section is assumed to be continuous, and the Finite Volume approach is applied to approximate homogeneous equations. Several suitable schemes to account for complex Equation Of State (EOS) are discussed namely : Rusanov scheme, an approximate form of Roe scheme, and VFRoe scheme with help of non conservative variables. In order to evaluate respective accuracy, the homogeneous Euler equations are computed first, and the L^1 error norm of transient solutions of shock tube experiments are plotted. It is shown that Rusanov scheme is indeed less accurate, which balances the fact that it enjoys interesting properties, since it preserves the positivity of the mean density, and the maximum principle for the vapour quality. Eventually, computations of real cases are presented, which account for mass transfer term, and time-space dependent cross sections.

1. INTRODUCTION

Some applications in industry require predicting flashing flows in variable cross section ducts. In some cases, it even becomes compulsory to account for cross sections which vary in time too, for instance when predicting flows in safety valves, which were one of the basic motivations of the following developments. From the modelling point of view, it is almost well admitted that the Homogeneous Relaxation Model is accurate enough to represent the true behaviour of that kind of flow. During past years, Bilicki and co-workers investigated such a kind of closures. For stationary one-dimensional flows, this model enables to predict the critical mass flow rate and the pressure distribution with a good accuracy[3-5, 16] . It requires some time scale to account for mass transfer which governs phase change in strong rarefaction waves. Friction effects will be disregarded herein, though they may be easily accounted for, without altering the global behaviour of the algorithm. This is due to the fact that the mean diameter of pipes in our applications is rather large. Present contribution actually aims at providing some ways to compute these complex industrial problems involving unsteady flashing flows, and more specifically giving some deep enough insight on the strength and weaknesses of three different upwinding techniques used in Finite Volume conservative schemes. We underline that emphasis is given on the latter schemes since they allow computation of any Equation Of State (EOS) on any kind of mesh.

We first describe the basics of the Homogeneous Relaxation Model (HRM), which governs the motion of the two phase mixture, assuming that relative velocities are small compared with the speed of acoustic waves in the medium, and have little influence on the whole behaviour of the flashing flows. Then, the overall numerical technique of reference[21] is briefly recalled, which relies on the Finite Volume method [19]. Special emphasis is given on three upwinding schemes to account for convective fluxes : an approximate Godunov [27] scheme (see [7-11, 23-24] , on the basis of initial proposition [25, 35]), and an extended version of Rusanov and Roe schemes [38-39, 18] to the frame of non conservative systems [6, 13, 15, 29] (see références [14, 32] for the theoretical framework). Some properties of schemes are recalled, and special emphasis is given on the true level accuracy (and the rate of convergence) obtained with the latter three, focusing on either steady flows in nozzles or on shock tube experiments involving gas, vapour or liquid and complex EOS. More precisely the L^1 error norm is plotted in various cases, which provides quantitative comparison which is seldomly available in the literature. This is one of the main contributions of the present work, which examines both steady and highly unsteady flow patterns. Eventually, we present an application of some two phase flashing flow in a nozzle ; this case is examined using the three different schemes. Though much important in practice, considerations about parallelizing of the code are not discussed herein, and the reader is referred to

références [2, 22] for such a matter. Some appendices provide more information on the way boundary conditions are handled [17] , and on the efficient VFRoe-ncv approximate Godunov scheme [7-11].

2. BASIC SET OF EQUATIONS

The basic set of equations of the Homogeneous Relaxation Model (noted HRM afterwards) consists in the following four equations, which govern the conservation laws for mass of the two-phase mixture, vapour phase, and total energy of both phases and an additional non conservative equation for the mean momentum. The whole writes [3, 4, 5, 16, 20, 33, 34] :

$$\begin{cases} \left(\rho S(x,t)\alpha\right)_{,t} + \left(\rho S(x,t) U \alpha\right)_{,x} = S(x,t)\Gamma \\ \left(\rho S(x,t)\right)_{,t} + \left(\rho S(x,t) U\right)_{,x} = 0 \\ \left(\rho S(x,t) U\right)_{,t} + \left(\rho S(x,t) U^2\right)_{,x} + S(x,t) P_{,x} = 0 \\ \left(S(x,t) E\right)_{,t} + \left(S(x,t)(E+P)U\right)_{,x} + P(S(x,t))_{,t} = 0 \end{cases} \tag{2.1}$$

when restricting to adiabatic flows. S(x,t) is the mean continuous cross section (otherwise, previous equations are meaningless), and is expected to be provided by users. ρ, U, P, α, E respectively stand for the mean density, the mean velocity, the mean pressure, the vapour quality (which is expected to lie in [0,1]), and the mean total energy of the two-phase mixture in the mean section. Subscripts ″t″ and ″x″ denote the time and space variables. The total energy of the two phase mixture is related to the internal energy as follows :

$$E = \rho \ e(\tau, \alpha, P) + \tfrac{1}{2}\rho u^2 \tag{2.2}$$

τ stands for the specific volume ($\tau = 1/\rho$). This must be supplemented by closure laws for the mass transfer term Γ, and for the total internal energy of the two-phase mixture e, which is given by :

$$e(\tau, \alpha, P) = \alpha \ e_{SV}(P) + (1-\alpha) \ e_{ML}\left(P, \frac{\tau - \alpha \ \tau_{SV}(P)}{1-\alpha}\right) \tag{2.3}$$

Subscripts ″ML″ and ″SV″ refer respectively to the metastable liquid and saturated vapour. Thermodynamic laws are given by Pollack [37].

Now an important issue when computing flashing flows concerns the forms for the mass transfer term. Bilicki and co-authors proposed some simplified form for this term :

$$\Gamma = -\rho \frac{\alpha - \overline{\alpha}}{\theta} \tag{2.4}$$

The mass transfer term requires computing the equilibrium quality :

$$\overline{\alpha} = \frac{h - h_{SL}(P)}{h_{SV}(P) - h_{SL}(P)} \tag{2.5}$$

where $h_{SL}(P)$ and $h_{SV}(P)$ respectively denote the specific enthalpy of the saturated liquid and the saturated vapour. Correlations used in computations for the time scale θ were given by Downar Zapolski and co-authors and are recalled in **appendix C**.

Before focusing on the numerical implementation of the model, we need to introduce some additional variables. Throughout the paper :

$$\hat{\gamma} = \frac{1}{\left(\frac{\partial e}{\partial P}\right)_{\tau,\alpha}} \left\{ \tau + \frac{\tau}{P} \left(\frac{\partial e}{\partial \tau}\right)_{P,\alpha} \right\} \tag{2.6}$$

and the square of the celerity of density waves is: $c^2 = \hat{\gamma}\ P\tau$. The specific entropy : $s = s\ (P, \tau, \alpha)$ is a function in agreement with :

$$\hat{\gamma}\ P \left(\frac{\partial s}{\partial P}\right)_{\tau,\alpha} - \tau \left(\frac{\partial s}{\partial \tau}\right)_{P,\alpha} = 0 \tag{2.7}$$

Hence the whole model is closed.

3. NUMERICAL METHOD

The numerical method is based on a fractional step technique [1, 13] , which allows computing time variations of the mean cross section, and the remaining of convective and source terms. The overall technique is detailed in référence [21]. It is shown therein that the splitting technique is in agreement with the whole entropy inequality. Even more, the computation of the PDE's in frozen duct (wrt time) still may be split into two steps : the first one involves the computation of the mass transfer term, and the second one deals with the homogeneous non conservative convective effects [14, 32]. Due to the ratio of the time scale associated with the fast acoustic waves over the time scale θ, which is smaller than one in practice, the fractional step approach is not penalized as may occur when computing other systems. In reference [21], it is shown that the specific form of the mass transfer term enables to ensure the maximum principle for the vapour quality for regular enough solutions. Details on numerical implementation of boundary conditions can be found in **appendix B** (see also [17,20] for further details). We thus only focus here on the comparison between three different ways to deal with convective terms. Alternative ways to deal with source terms, including a comparison with techniques suggested in [36] can be found in reference [20].

The main two steps are the following. Given some time step Δt^n, and initial data $\mathbf{W^n}$ at time t^n , one computes the following ODE for given mean values of $\mathbf{W_i^n}$ over cell « i »

$$\mathbf{W_i^n} = \int_{\Omega_i} \mathbf{W}\left(x, t^n\right) dx \Big/ h_i$$

The time step is chosen in agreement with some CFL condition, and h_i is the mesh size of cell « i ». Hence :

Step 1 :

$$\begin{cases} \left(\rho S(x,t)\alpha\right)_{,t} = S(x,t)\Gamma \\ \left(\rho S(x,t)\right)_{,t} = 0 \\ \left(\rho S(x,t)U\right)_{,t} = 0 \\ \left(S(x,t)E\right)_{,t} + P\left(S(x,t)\right)_{,t} = 0 \\ \left(S(x,t)\right)_{,t} = j(x,t) \end{cases} \tag{3.1}$$

provides on each cell « i » of the mesh :

$$\tilde{\mathbf{W}}_\mathbf{i} = \psi_1\left(\left\{\mathbf{W_k^n}\right\}_{k\in Z}\right)$$

Obviousy, this step is skipped when the cross section does not vary with time (j(x,t)=0). We recall that the mean velocity and the specific entropy do not vary through this step. The vapour quality and the mean density agree with :

$$\alpha_{,t} = \frac{\Gamma}{\rho}$$

$$\left(\mathrm{Log}\rho\right)_{,t} = -\frac{j}{S}$$

Once step 1 is solved, the convective system is solved over the time interval $[t^n , t^n + \Delta t^n]$, given initial data $\tilde{\mathbf{W}}_i^n$ on each cell, and suitable boundary conditions :

Step 2 :

$$\begin{cases} \left(\rho S(x,t)\alpha\right)_{,t} + \left(\rho S(x,t)\alpha U\right)_{,x} = 0 \\ \left(\rho S(x,t)\right)_{,t} + \left(\rho S(x,t)U\right)_{,x} = 0 \\ \left(\rho S(x,t)U\right)_{,t} + \left(\rho S(x,t)U^2\right)_{,x} + S(x,t)P_{,x} = 0 \\ \left(S(x,t)E\right)_{,t} + \left(S(x,t)(E+P)U\right)_{,x} = 0 \\ \left(S(x,t)\right)_{,t} = 0 \end{cases} \tag{3.2}$$

which provides on each cell « i » of the mesh :

$$\mathbf{W_i^{n+1}} = \psi_2\left(\left\{\tilde{\mathbf{W}}_\mathbf{k}\right\}_{k\in Z}\right)$$

Details pertaining to Riemann invariants of the homogeneous part of step 2, on shock relations, and on positivity constraints through the one dimensional Riemann problem associated with the latter system are recalled in a previous paper [21]. The source term may be computed with an extra fractional step method. This may be done in the simplest following way (which preserves the maximum principle for the vapour quality at a discrete level), by computing $\alpha(t+\Delta t)$ as a function of $\alpha(t)$ as :

$$\alpha(t+\Delta t) = \exp\left(\frac{-\Delta t}{\theta(t)}\right)\alpha(t) + (1-\exp\left(\frac{-\Delta t}{\theta(t)}\right))\overline{\alpha}(t) \tag{3.3}$$

or either using interface values of state variables. We from now on discuss upwinding techniques.

4. UPWINDING TECHNIQUES.

We will now focus on the computation of the convective system (step 2) using three different schemes ; the three of them enable to handle complex thermodynamic laws. The convective system (3.2) may be written under a condensed form :

$$(S\mathbf{W})_{,t} + \left(S\mathbf{F(W)}\right)_{,x} + S\mathbf{G(W)}_{,x} = \mathbf{0} \tag{4.1}$$

where **W** is the physical « convervative » variable. The flux functions are given by :

$$\mathbf{F(W)^t} = \left(\rho U\alpha, \rho U, \rho U^2, U(E+P)\right) \tag{4.2.a}$$

$$\mathbf{G(W)^t} = \left(0,0,P,0\right) \tag{4.2.b}$$

The basic idea is then the following. The given section of the duct is discretized, and is assumed to be piecewise linear on each interface of control volumes. Besides, we introduce constant reconstruction of the ″conservative″ variable :

$$\mathbf{W}^t = \left(\rho\alpha, \rho, \rho U, E\right) \tag{4.3}$$

over cell i. Hence :

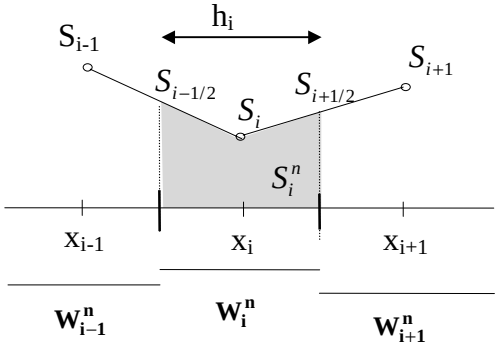

Given some approximate values of the cross section at the cell centre S at time t^n, the cross section at the interface is defined using a linear interpolation :

$$S_{i+1/2} = \frac{h_i S_{i+1} + h_{i+1} S_i}{h_i + h_{i+1}} \tag{4.4}$$

The mean value of S(x)over cell Ω_i is given by :

$$\widehat{S}_i = \int_{\Omega_i} S\left(x, t^n\right) dx \Big/ h_i \tag{4.5.a}$$

or :

$$\widehat{S}_i = S_i\left(1 - \frac{h_i}{4\left(h_i + h_{i+1}\right)} - \frac{h_i}{4\left(h_i + h_{i-1}\right)}\right) + \frac{h_i}{4}\left(\frac{S_{i-1}}{h_i + h_{i-1}} + \frac{S_{i+1}}{h_i + h_{i+1}}\right) \tag{4.5.b}$$

All schemes will take the form :

$$h_i \widehat{S}_i \left(\mathbf{W_i^{n+1}} - \widetilde{\mathbf{W}}_\mathbf{i} \right) + \Delta t^n \widehat{S}_i \left(G_{i+1/2}{}^{\text{scheme}} - G_{i-1/2}{}^{\text{scheme}} \right) + \Delta t^n \left\{ S_{i+1/2} \mathbf{F}_{i+1/2}{}^{\text{scheme}} - S_{i-1/2} \mathbf{F}_{i-1/2}{}^{\text{scheme}} \right\} = \mathbf{0}$$

We define below various forms of numerical fluxes $\mathbf{F}^{\mathbf{scheme}}$ and $\mathbf{G}^{\mathbf{scheme}}$. These formulas should provide consistant and stable approximation of fluxes in the sense of [19]. We use the standard notation :

$$\overline{\phi}_{i+1/2} = \frac{\phi_i + \phi_{i+1}}{2}$$

4.1 Rusanov scheme

An extension of the original Rusanov scheme [39] yields :

$$\left(G^{\text{Rusanov}}{}_{i+1/2} \right)^t = \left(0 \ , 0 \ , \widetilde{\overline{P}}_{i+1/2} , \ 0 \ \right) \tag{4.6}$$

$$\mathbf{F}^{\textit{Rusanov}}{}_{\mathbf{i+1/2}} \left(\widetilde{\mathbf{W}}_\mathbf{i} , \widetilde{\mathbf{W}}_{\mathbf{i+1}} \right) = \frac{1}{2} \left\{ \mathbf{F} \left(\widetilde{\mathbf{W}}_\mathbf{i} \right) + \mathbf{F} \left(\widetilde{\mathbf{W}}_{\mathbf{i+1}} \right) - \widehat{s}_{i+1/2} \left(\widetilde{\mathbf{W}}_{\mathbf{i+1}} - \widetilde{\mathbf{W}}_\mathbf{i} \right) \right\} \tag{4.7}$$

where :

$$\widehat{s}_{i+1/2} = \max \left(\left| \widetilde{u}_i \right| + \widehat{c}_i \ , \ \left| \widetilde{u}_{i+1} \right| + \widehat{c}_{i+1} \right) \tag{4.8}$$

noting the numerical sound velocity :

$$\hat{c}_i^2 = \widetilde{\widehat{\gamma}}_i \ \widetilde{P}_i \ \widetilde{\tau}_i \tag{4.9}$$

Recall that one of the main advantages of Rusanov scheme is that it ensures the positivity of the density, and the discrete maximum principle for the vapour quality provided that some CFL condition holds (see **appendix A**).

4.2 An approximate form of Roe scheme

In a somewhat different framework, an extension of the original Roe scheme to the frame of non-conservative systems was proposed in [29]. This one enables to handle time dependent and stationary flows. We use herein a slightly modified version of the scheme (see also [6]), which does not require consistancy with the integral form of the conservation law -as standard Roe scheme does-, and is thus useful when dealing with complex EOS. For convenience, we define :

$$\mathbf{B}(\mathbf{W}) = \frac{\partial \mathbf{F}(\mathbf{W})}{\partial \mathbf{W}} + \frac{\partial \mathbf{G}(\mathbf{W})}{\partial \mathbf{W}} \tag{4.10}$$

and introduce :

$$\mathbf{F}^{\mathrm{Roe}}{}_{i+1/2}\left(\tilde{\mathbf{W}}_i, \tilde{\mathbf{W}}_{i+1}\right) = \frac{1}{2}\left\{\mathbf{F}\left(\tilde{\mathbf{W}}_i\right) + \mathbf{F}\left(\tilde{\mathbf{W}}_{i+1}\right) - \left|\mathbf{B}\ \left(\hat{\mathbf{W}}\left(\tilde{\mathbf{Y}}_i, \tilde{\mathbf{Y}}_{i+1}\right)\right)\right|\left(\tilde{\mathbf{W}}_{i+1} - \tilde{\mathbf{W}}_i\right)\right\} \tag{4.11}$$

noting :

$$\left|\mathbf{B}\ \left(\hat{\mathbf{W}}\left(\tilde{\mathbf{Y}}_i, \tilde{\mathbf{Y}}_{i+1}\right)\right)\right| = \mathbf{\Omega}\left(\hat{\mathbf{W}}\left(\tilde{\mathbf{Y}}_i, \tilde{\mathbf{Y}}_{i+1}\right)\right)\ \left|\mathbf{\Lambda}\left(\hat{\mathbf{W}}\left(\tilde{\mathbf{Y}}_i, \tilde{\mathbf{Y}}_{i+1}\right)\right)\right|\ \left(\mathbf{\Omega}\left(\hat{\mathbf{W}}\left(\tilde{\mathbf{Y}}_i, \tilde{\mathbf{Y}}_{i+1}\right)\right)\right)^{-1} \tag{4.12}$$

and :

$$\mathbf{B}\ (\mathbf{W}) = \mathbf{\Omega}(\mathbf{W})\ \ \mathbf{\Lambda}(\mathbf{W})\ \left(\mathbf{\Omega}(\mathbf{W})\right)^{-1} \tag{4.13}$$

Matrix $\mathbf{\Omega}(\mathbf{W})$ represents the matrix of right eigenvectors of matrix **B**(**W**) introduced in (4.10) ; associated matrix $\mathbf{\Lambda}(\mathbf{W})$ is the diagonal matrix containing ordered eigenvalues :

$$\lambda_1 = U - c \qquad \lambda_2 = \lambda_3 = U \qquad \lambda_4 = U + c$$

Eventually : $\left|\mathbf{\Lambda}\left(\hat{\mathbf{W}}\right)\right|_{kk} = \left|\lambda_k\left(\mathbf{\Lambda}\left(\hat{\mathbf{W}}\right)\right)\right|$. The mean value of the conservative state is defined as :

$$\hat{\mathbf{W}}\left(\tilde{\mathbf{Y}}_i, \tilde{\mathbf{Y}}_{i+1}\right) = \mathbf{W}\left(\frac{\tilde{\mathbf{Y}}_i + \tilde{\mathbf{Y}}_{i+1}}{2}\right) \tag{4.14}$$

where variable Y is defined as $\mathbf{Y}^t = (\alpha, \tau, u, P)$. Note that $G^{\mathrm{Roe}}{}_{i+1/2}$ is still given as :

$$\left(G^{\mathrm{Roe}}{}_{i+1/2}\right)^t = \left(0\ ,0\ ,\tilde{\tilde{P}}_{i+1/2},\ 0\ \right) \tag{4.15}$$

This scheme has been extensively used to predict the behaviour of second order turbulent closures in single phase flows, when no Roe's average is available [6]. We emphasize that this scheme does not ensure the positivity of density and the maximum principle for vapour quality of cell values. We recall that the original Roe scheme, which requires satisfying so-called Roe's condition (or in other words consistency with the integral form of the conservation law) only ensures positivity of density and mass fraction of vapour on -one dimensional- « staggered grid » (namely fictitious cell $[x_i, x_{i+1}]$), whereas exact Godunov scheme enables preservation of : $\rho \geq 0$, $1 \geq \alpha \geq 0$ on cell values, owing to the projection of exact solution on the mesh .

4.3 An approximate Godunov scheme : VFRoe scheme with non conservative variable.

The original VFRoe scheme is an approximate Godunov scheme which was first introduced in [25, 35]. VFRoe-ncv scheme is a sequel of the latter which generalizes the approach by requiring some invertible change of variable, which provides so-called non conservative variable Y(W). The scheme was introduced in [7] , with applications to shallow water equations including comparison with the basic Godunov scheme [8], and applications to Euler gas dynamics with arbitrary EOS in [9]. Some possible extensions to the frame of non conservative hyperbolic systems were defined and discussed in [10-11].

Appendix D gives a description which permits straightforward coding of the scheme . A recent note [23] gives some detailed comparison of capacities of the scheme with comparison with the energy relaxation method [30], the Rusanov scheme, and Toro PVRS scheme [41]. It also provides the main properties of the scheme when restricting to pure shock waves, steady or unsteady contact discontinuities, retaining simple EOS such as perfect gas EOS, Tamman EOS, or more sophisticated ones including stiffened gas EOS, Van der Waals EOS, Chemkin database or tabulated laws (see [24]). The field of practical applications of VFRoe-ncv scheme up to now has mainly concerned gas flows in turbines, in laminar and turbulent situations. We recall that fluxes are given by :

$$\left(G^{\text{VFRoencv}}{}_{i+1/2}\right)^t = \left(0\ ,0\ ,P^*_{i+1/2},\ 0\ \right) \tag{4.16}$$

$$\mathbf{F}^{\text{VFRoencv}}{}_{\mathbf{i+1/2}}\left(\tilde{\mathbf{W}}_{\mathbf{i}}, \tilde{\mathbf{W}}_{\mathbf{i+1}}\right) = \mathbf{F}\left(\mathbf{W}\left(Y^*_{i+1/2}\right)\right) \tag{4.17}$$

The starred value at interface $Y^*_{i+1/2}$ is obtained by solving a linear hyperbolic problem (**see appendix D).** We only provide below specific properties of the scheme when applying for $\mathbf{Y}^{\mathbf{t}} = (\alpha, \tau, U, P)$ « non conservative » variable. The first one concerns intermediate states of both pressure and velocity variables in the linearized Riemann solver at interface. Denoting P_1 and P_2 (respectively U_1 and U_2) values of pressure (respectively velocity) on left side and right side of the contact discontinuity associated with eigenvalue U, one may easily check that (see **appendix D**) :

$$P_1 = P_2$$
$$U_1 = U_2$$

Moreover, we may check that :

$$\alpha_1 = \alpha_i\,, \alpha_2 = \alpha_{i+1}\,.$$

Thus approximate values of the vapour quality at the interface predicted by VFRoe-ncv scheme are « exact » in the sense that they mimic the numerical values predicted by the exact Godunov scheme (the 1-wave and the 4-wave are ghost waves for vapour quality in the exact solution of the Riemann problem). Obviously the maximum principle for the vapour quality holds true.

5. NUMERICAL RESULTS

System (2.1) admits solutions which may be discontinuous. Moreover time scales associated with relaxation mass transfer terms and convective terms may be completely different ; this may render computations rather tricky especially when the time scale associated with the relaxation term is small compared with the numerical time step imposed by the CFL condition in relation with convective effects. Fortunately, physical effects involved here are in favour of the fractional step method. Sudden variations of the cross section (for instance when computing safety valves) may in addition penalize accuracy in some configurations. Extensive validation of VFRoe-ncv scheme has been previously performed when focusing on real gas flows and considering several EOS [7-11]. The efficiencies of the Rusanov scheme and the approximate Roe type Riemann solver have been investigated in a different framework (see [23 , 6]). When restricting to Euler equations of gas dynamics with perfect gas EOS, and focusing on the computation of shock tube experiments with so called first-order scheme, the rate of convergence (measuring error in L^1 norm) is ½ for the concentration of pollutant (which does not vary in the Genuinely Non Linear fields), and 1 for velocity and pressure (which do not change through the contact discontinuity). Figure 1 shows the evolution of the error for the concentration using either « first » order or « second » order scheme (in the latter case, the rate grows up to 2/3). In all cases the discrete error at time T is computed using a regular mesh according to :

$$\left\|\phi - \phi_h\right\|(h,T) = \frac{\sum_{i=1}^{N} \left|\phi_h(x_i,T) - \phi\ (x_i,T)\right|}{\sum_{i=1}^{N} \left|\phi\ (x_i,T)\right|}$$

The rate of convergence for given value of CFL number is β provided that the error follows the law :

$$\left\|\phi - \phi_h\right\|(h,T) = C(\phi,T)h^{\beta}$$

when h tends to 0 . We below restrict to the first order version of the scheme.

5.1 Steady flow in a nozzle filled with perfect gas.

The fluid is assumed to be represented by perfect gas EOS. Subsonic inlet and outlet boundary conditions are imposed so that a shock is present in the divergent part of the nozzle. Initial conditions are :

$$P = 8 \text{ bar},\ T = 400° \text{ K},,\ \alpha = 1,\ U = 0 \text{ m/s}.$$

Boundary conditions are :

$$P_{inlet} = 10 \text{ bar}, \quad \alpha_{inlet} = 1, \quad (\rho SU)_{inlet} = 1504 \text{ kg/s}$$

$$P_{outlet} = 8 \text{ bar}$$

First three figures (figure 2) provide the rate of convergence of schemes towards the exact **steady** solution. We focus here on the mean pressure, the Mach number and the mass flow rate. The rate of convergence is close to 1^- for all variables and for all schemes. Comparing Rusanov and VFRoe scheme, it appears that VFRoe provides the same accuracy using a mesh size h instead of h/8. Other examples are available in [20].

5.2 Steady flow in a nozzle filled with real gas.

We use here similar initial and boundary conditions but apply for real gas EOS. Figure 3 shows that Rusanov scheme does not provide a sharp (steady) shock profile in the divergent part when using a coarse mesh with two hundred nodes. The numerical prediction of the **steady** mass flow rate (ρ U S) is much better predicted when using VFRoe scheme. We emphasize that we have plot here cell values of mass flow rate but not interface mass fluxes. Hence, Roe scheme and Rusanov scheme predict a slightly different value than expected. These discrepancies tend towards zero when the mesh is refined. The small glitch (which tends to 0 when the mesh is refined) around the shock location when using VFRoe scheme is due to numerical perturbations coming from subsonic outflow which interact with the numerical shock profile ; this is combined with the fact that VFRoe-ncv scheme does not satisfy « Roe's condition » (or in other words consistency with the integral form of the conservation law) for complex EOS (see [7,9]). We note too that the amplitude of this glitch is small compared with the difference between constant values predicted by Roe and Rusanov schemes and expected value imposed by user at the inlet boundary. The relative error computed on the basis of the mass flow rate at interfaces predicted by VFRoe scheme (see appendix D) is much lower than cell values of mass flow rate on given mesh size (which means that the flow is steady at a discrete point of view). Similar comments hold for cell values and interface values for the total enthalpy $H=(E+P)/\rho$. The most accurate prediction is given here by VFRoe scheme.

5.3 SOD shock tube with liquid water.

Shock tube tests simulate the solution of the Riemann Problem with constant cross section $S(x)=S_0$. Thus they are very useful to study the capabilities of schemes to compute transient flows. Physically speaking, they correspond to the following situation : a membrane, which initially separates two fluids with different thermodynamic states, is suddenly broken, so that waves start to propagate.

Initial conditions for the first shock tube test case are detailed below (subscripts L and R still refer to the left hand side and the right hand side of the membrane) :

$$P_L = 2000 \text{ bar}, \rho_L = 1017.8 \text{ kg/m}^3, \alpha_L = 1, \text{ and } u_L = 0 \text{ m/s}$$

$$P_L = 100 \text{ bar}, \rho_R = 838.3 \text{ kg/m}^3, \alpha_R = 1, \text{ and } u_R = 0 \text{ m/s}$$

Under these conditions a shock wave travels to the right, followed by a contact discontinuity, while a rarefaction wave propagates to the left.

We have plot L^1 error of predicted approximations provided by the three schemes using CFL number 0.95 (figure 4). The measured rate of convergence is approximately the same for both velocity and pressure variables for both VFRoe-ncv and Roe type schemes : $\delta_U = \delta_P = 0.85$. It is thus close to the expected value of 1 (the « second order » version of the scheme enables to reach rate 1^- on similar meshes). Part of the discrepancy is linked with the fact that the EOS is complex so that some error around the contact discontinuity is introduced (see [24]), which slows down the convergence on these rather « coarse » meshes. Meanwhile the rate of convergence for the density is around : $\delta_\rho = 0.65$, and thus still a bit greater than expected value of ½ when h tends to 0. This is due to occurrence of variations of the density in the 1-rarefaction wave and through the 3-shock wave, which contribute to a balance between order ½ and 1 on intermediate mesh sizes. This is confirmed by the measured rate of convergence of density for Rusanov scheme which is approximately $\delta_\rho = 0.52$ instead of expected ½. Actually, in order to reach the same accuracy, one needs almost twice the number of cells when using Rusanov scheme instead of Roe scheme (or VFRoe scheme).

5.4 SOD shock tube with vapour.

Initial conditions for the second shock tube tests case are given :

$$P_L = 5 \text{ bar}, \rho_L = 2.215 \text{ kg/m}^3, \alpha_L = 1, \text{ and } u_L = 0 \text{ m/s}$$

$$P_R = 1 \text{ bar}, \rho_R = 0.435 \text{ kg/m}^3, \alpha_R = 1, \text{ and } u_R = 0 \text{ m/s}$$

The CFL number is still 0.95. Similar comments hold here as in the previous case (figure 5). Nonetheless, the performances for complex EOS around the contact discontinuity are better owing to the behaviour which in practice is very similar to the one associated with use of perfect gas EOS. The measured rate of convergence is still the same for both velocity and pressure for both VFRoe-ncv and Roe type schemes, and is around: $\delta_U = \delta_P = 0.9$, instead of expected value 1. The rate of convergence for the density is once more : $\delta_\rho = 0.65$ (instead of ½) . There are indeed very few differences between rates of convergence of the three schemes here, but Rusanov scheme is still less accurate than the other two on given mesh size.

5.5 Flashing flow in a nozzle.

Initial conditions in the duct are:

$$P = 15 \text{ bar}\,,\ T = 470 \text{ K}\,,\ \rho = 874{,}3 \text{ kg} / \text{m}^3,\ \alpha = 0\,,\ u = 0 \text{ m} / \text{s}\,.$$

At the beginning of the computation, the pressure at the outflow suddenly decreases to :

$$P_{out} = 10 \text{ bar}$$

The regular mesh contains 1000 nodes ($h=10^{-3}$m). The CFL number has been set to 0.9. Figure 6 shows the pressure distribution, the velocity distribution, and the void fraction distribution along the pipe due to rarefaction wave travelling to the left. Similar computations involving higher pressure ratios are reported in reference [22]. The three schemes behave in a similar way, and there is indeed no contradiction with previous results, since no shock wave nor contact discontinuity is present in the flow field here, unlike in previous cases of unsteady shock tube experiments. Nonetheless we may notice some differences between results close to the right boundary condition where the vapour quality varies strongly.

6. CONCLUSION

Several ways to compute unsteady flashing flows in variable cross section ducts have been summarised in this paper, on the basis of an approximate Godunov scheme called VFRoe-ncv, an approximate form of Roe 's scheme and the early Rusanov scheme. All behave rather well ; nonetheless, Rusanov scheme suffers from a rather great amount of diffusion, which penalizes the scheme accuracy when computing steady or unsteady flows including shock waves. One of the main contribution concerns investigation of the true rate of convergence and of the level of accuracy for given mesh size. Focusing on pressure and velocity variables (respectively the density and the vapour quality), standard MUSCL type extension combined with second order Runge-Kutta time integration (which was not discussed herein) enables to reach first order convergence rate on rather coarse -or industrial- meshes (respectively rate of convergence of 2/3) when computing unsteady shock tube experiments, and second order when predicting regular flows (see [8, 9, 20, 22, 23]). The code is currently used in our company for practical purposes involving safety valves loaded with pressurised vapour or liquid (see [22]). The field of applications of the Homogeneous Relaxation Model is obviously rather wide in the industry. In all cases involving liquid water, or a mixture of vapour and liquid, it was noted that requiring sufficient small amount of error results in the use of very fine meshes, even in the one dimensional framework. Actually, in some cases, a mesh with approximately ten thousand nodes may be compulsory ; otherwise coarser meshes may provide unrealistic prediction which are not converged with respect to the mesh size (see [22]). Though not totally sufficient from a theoretical point of view, this is currently overcome using parallel versions of the code, which turns to be a rough though efficient way to handle the situation (see [2]). All computations up to now have benefited from the fact that time scales associated with mass transfer terms and convective effects are in favour of the use of the fractional step technique. Some difficulties have nonetheless arisen in some cases when flashing phenomena occurs close to some boundary condition. The strong coupling between non linear effects of convection and sources, but also on the -non linear- computation of local thermodynamic properties renders the analysis of encountered slow down of convergence cumbersome. The smearing of the -slow- contact discontinuity by upwinding schemes, or in other words the poor accuracy around the latter Linearly Degenerate field, which in addition supports the jump of the vapour quality and of the mean density, may lead to non linear interactions in EOS, and yield blow up of code when the mesh is too coarse. The only remedy sometimes is obtained by local refining of the mesh.

On the whole, these show that the development and progress on algorithm improvements in at least three distinct directions are still mandatory. A first point concerns the treatment of contact

discontinuities in conservative schemes using upwinding techniques, in order to minimise error around the latter, especially when complex EOS are involved. Several attempts in that direction have now been already done (see [24, 31] among others). Another tricky problem is related to the different time scales associated with velocity of the fluid and the sound speed in almost incompressible fluids ; this is indeed clearly related to the standard problem of preconditioning of compressible algorithms in flows with low speed patterns (see [12 , 42, 43]). A third important point is connected with the coupling of source terms in convection dominated flows ; this is particularly important in flows which may involve stiff source terms due to mass transfer. Progress has been made in that field too (see [28, 36] for instance), but it still deserves more thinking. Up to the authors, the whole means that 3D computations of the HRM model with sufficiently fair accuracy are almost beyond the reach of current computer facilities provided by local work stations.

Acknowledgments :

Reviewers are acknowledged for their suggestions for changes which helped improve the early version of the manuscript. Authors would indeed like to thank Laurent Scliffet who used to manage the MORSE project and encouraged these developments. We are also greatful to Pr Thierry Gallouet for his continuous support and nice effort in helping us through encountered difficulties. Computational facilities have been provided by EDF (Electricité de France) - Division Recherche Développement. Second author has benefited from financial support from EDF during his PhD thesis.

7. REFERENCES

[1] Baraille R., Bourdin G., Dubois F., and Leroux A.Y. « Une version à pas fractionnaires du schéma de Godunov pour l'hydrodynamique» *Comptes Rendus Académie des Sciences Paris* , I-314, 1992, pp. 147-152.

[2] Berthou J.Y., and Fayolle E. « Parallélisation de la version industrielle du code HRM1D : ECOSS » EDF report HI-76/00/016/A, Electricite de France. Division Recherche Développement, 6 quai Watier 78400 Chatou, France, 2000.

[3] Bolle L., Downar-Zapolski P., Franco J., and Seynhaeve J.M. « Experimental and Theoretical Analysis of Flashing Water through a Safety Valve » *International Symposium on Heat and Mass Transfer in Chemical process Industry Accidents,* September 15-16, 1994, Rome, Italy

[4] Bilicki Z., and Kardas D. « Approximation of thermodynamic properties for subcooled water and superheated steam » Polish Academy of Sciences, Institute for Fluid Flow Machinery, Gdansk, Poland, Nr. Arch. 185/91 , 1991.

[5] Bilicki Z., Kestin J., and Pratt M.M. « A reinterpretation of the results of the Moby-Dick experiments in terms of the nonequilibrium model » *Journal of Fluids Engineering* , vol.112, 1990, pp 212-217.

[6] Brun G., Hérard J.M., Jeandel D., and Uhlmann M. « An approximate Roe-type Riemann solver for a class of realizable second order closures » *Journal of Computational Physics,* vol. 151 , n 2 , 1999, pp. 990-996.

[7] Buffard T., Gallouët T., and Hérard J.M. « Schéma VFRoe en variables caractéristiques. Principe de base et application aux gaz réels » EDF report HE-41/96/041/A, in French. Electricite de France. Division Recherche Développement, 6 quai Watier 78400 Chatou, France, 1996.

[8] Buffard T., Gallouët T., and Hérard J.M. « A naive scheme to solve shallow water equations» *Comptes Rendus Académie des Sciences Paris* , I-326, 1998, pp. 385-390.

[9] Buffard T., Gallouët T., and Hérard J.M. « A sequel to a rough Godunov scheme. Application to real gases » *Computers and Fluids,* vol. 29, n°7, 2000, pp. 813-847.

[10] Buffard T., Gallouët T., and Hérard J.M. « A naive Riemann solver to compute a non conservative hyperbolic system » *International Series on Numerical Mathematics,* vol. 129, 1999, pp. 129-138 .

[11] Buffard T., Gallouët T., and Hérard J.M. « An approximate Godunov scheme to compute turbulent real gas flow models» *AIAA paper 99-3349* , 1999.

[12] Clerc S. « Etude des schémas décentrés implicites pour le calcul numérique en mécanique des fluides. Résolution par décomposition de domaine» PhD Thesis, Université Paris VI, Paris, France , November 7, 1997.

[13] Combe L., and Hérard J.M. « A Finite Volume algorithm to compute dense compressible gas-solid flows» *AIAA Journal* , vol. 37, n°3, 1999, pp. 335-342.

[14] Dal Maso G. , Le Floch P.G , and Murat F. « Definition and weak stability of non conservative products» *Journal de Mathématiques Pures et Appliquées,* vol. 74, 1995, pp. 483-548.

[15] Declercq E., Forestier A., Hérard J.M., Louis X., and Poissant G. « An exact Riemann solver for a multicomponent turbulent compressible flow» *International Journal of Computational Fluid Dynamics* , to appear.

[16] Downar-Zapolski P., Bilicki Z., Bolle L., and Franco J. « The non-equilibrium model for one-dimensionnal flashing liquid flow » *International Journal of Multiphase Flow* 22, 196, pp 473-483.

[17] Dubois F. « Boundary conditions and the Osher scheme for the Euler equations of gas dynamics » CMAP report n°170 , Centre de Mathématiques Appliquées de l'Ecole Polytechnique, Palaiseau, France, 1987.

[18] Einfeldt B ., Munz C.D., Roe P.L., and Sjogreen B. « On Godunov type methods near low densities » *Journal of Computational Physics,* vol. 92-2, 1991, pp. 273-295.

[19] Eymard R., Gallouët T., and Herbin R., « *Finite Volume methods* » Handbook for Numerical Analysis, P.G. Ciarlet and J.L. Lions editors, North Holland, vol. 7, 2000, pp . 729-1020.

[20] Faucher E. , « Simulation numérique d'écoulements unidimensionnels instationnaires avec auto vaporisation » PhD thesis , IUT Melun Sénart, January 24, 2000.

[21] Faucher E., Herard J. M., Barret M., and Toulemonde C. « Computation of flashing flows in variable cross section ducts » » *International Journal of Computational Fluid Dynamics,* vol. 13, n°3, 2000, pp. 365-391.

[22] Faucher E., Herard J. M., Levu G., and Scliffet L. « Simulation numérique d'écoulements diphasiques eau-vapeur. Application à l'APRP et à quelques problèmes de fonctionnement de soupape » internal EDF report HE-41/99/037/A, in French. Electricite de France. Division Recherche Développement, 6 quai Watier 78400 Chatou, France, 1999.

[23] Gallouët T., Herard J.M., and Seguin N « Some recent Finite Volume schemes to compute Euler equations using real gas EOS » preprint LATP 00-021, Centre de Mathématique et d'Informatique, Université de Provence 13453 Marseille, France , 2000.

[24] Gallouët T., Herard J.M., and Seguin N «An hybrid scheme to compute contact discontinuities in Euler systems » internal EDF report HI-81/01/011/A, . Electricite de France. Division Recherche Développement, 6 quai Watier 78400 Chatou, France, 2001.

[25] Gallouët T., and Masella J.M., « A rough Godunov scheme » *Comptes Rendus Académie des Sciences Paris* , I-323, 1996, pp.77-84.

[26] Godlewski E., and Raviart P.A. « *Numerical analysis for hyperbolic systems of conservation laws* » Springer Verlag , 1997.

[27] Godunov S.K. « A finite difference method for the numerical computation of discontinuous solutions of the equations of fluid dynamics » *Math. Sb.* , vol; 47, 1959, pp. 217-300 .

[28] Greenberg J.M., and Le Roux A.Y. « A well balanced scheme for the numerical procesing of source terms in hyperbolic equations» *SIAM Journal of Numerical Analysis.* , vol. 33, n°1, 1996, pp. 1-16.

[29] Herard J. M. « Solveur de Riemann approché pour un système hyperbolique non conservatif issu de la turbulence compressible » in French, EDF report HE-41/95/009/A , Electricite de France. Division Recherche Développement, 6 quai Watier 78400 Chatou, France , 1995.

[30] In A., « Numerical evaluation of an energy relaxation method for inviscid real fluids » *SIAM Journal of Scientific Computing*, vol. 21-1, 19999, pp. 340-365 .

[31] Karni S, « Multi component flow calculations by a consistent primitive algorithm » *Journal of Computational Physics*, vol. 112, 1994, pp. 31-43 .

[32] Le Floch P.G. « Entropy weak solutions to non linear hyperbolic systems in non conservative form » *Communications. In Partial Differential Equations* , Vol. 13-6, 1996, pp. 669-727.

[33] Lemaire C. « Caractérisation et modélisation du blocage de débit en écoulement dispersé à deux constituants en géométrie tridimensionnelle» PhD thesis, Grenoble, France , November 10 , 1999.

[34] Lemaire C., Lemonnier H., and Dehais G. « Determination of two-phase critical flow : implementation and assessment of a reference technique » *36th European Two-Phase Flow Group Meeting, 1st European-Japanese Two-Phase Flow Group Meeting*, Portoroz, Slovenie, 1-2 june , 1998 .

[35] Masella J.M., Faille I., and Gallouët T. « On a rough Godunov scheme » *International Journal of Computational Fluid Dynamics*, vol. 12, 1999, pp. 133-149 .

[36] Papalexandris M. V., Leonard A., and Dimotakis P.E. « Unsplit schemes for hyperbolic conservation laws with source terms in one space dimension» *Journal of Computational Physics*, vol. 134, 1997, pp. 31-61.

[37] Pollack R. « Die thermodynamischen Eigenschaften von Wasser dargestellet durch eine kanonische zustands gleichung fur die fluiden homogenen and heterogenen zustande bis 1200 Kzlvin und 3000 bars » Dissertation Ruhr Universitat , 1974.

[38] Roe P.L. « Approximate Riemann solvers, parameter vectors and difference schemes » *Journal of Computational Physics* , vol. 43, 1981, pp 357-372 .

[39] Rusanov V.V. « The calculation of the interaction of non-stationary shock waves and obstacles » *Zh. Vich. Nat.* , n°2, 1961, pp. 304-320 .

[40] Smoller J. . « *Shock waves and reaction-diffusion equations* » Springer-Verlag , 1983.

[41] Toro E.F. « *Riemann solvers and numerical methods for fluid dynamics* » Springer-Verlag , 1997.

[42] Turkel E. « Preconditioned methods for solving the incompressible and low speed compressible equations » *Journal of Computational Physics*, vol.72, 1987, pp. 277-298.

[43] Turkel E. « Review of preconditioned methods for fluid dynamics » *Applied Numerical Math*ematics, vol.12, 1993 , pp. 257-284 .

Appendix A

We examine here whether the maximum principle holds for the approximate values of the vapour quality, when using Rusanov scheme. Focusing on mass conservation first, we get :

$$\begin{aligned}\widehat{S}_i h_i \rho_i^{n+1} &= \rho_i^n \left\{ \widehat{S}_i h_i - \frac{\Delta t}{2} \left\{ \widehat{S}_{i+1/2} \left(s(W_i^n, W_{i+1}^n) + U_i^n \right) + \widehat{S}_{i-1/2} \left(s(W_{i-1}^n, W_i^n) - U_i^n \right) \right\} \right\} \\ &+ \frac{\Delta t}{2} \left(s(W_i^n, W_{i+1}^n) - U_{i+1}^n \right) \widehat{S}_{i+1/2} \rho_{i+1}^n + \frac{\Delta t}{2} \left(s(W_{i-1}^n, W_i^n) + U_{i-1}^n \right) \widehat{S}_{i-1/2} \rho_{i-1}^n \end{aligned} \tag{A1}$$

Thus noting that :

$$\begin{aligned} s(W_i^n, W_{i+1}^n) - U_{i+1}^n \geq 0 \\ s(W_{i-1}^n, W_i^n) + U_{i-1}^n \geq 0 \end{aligned} \tag{A2a}$$

$$\begin{aligned} s(W_i^n, W_{i+1}^n) + U_i^n \geq 0 \\ s(W_{i-1}^n, W_i^n) - U_i^n \geq 0 \end{aligned} \tag{A2b}$$

owing to the definition of $s(W_i, W_{i+1})$ (maximum value of the spectral radius of Jacobian matrix on cell i and « i+1 »), we immediately conclude that the mean density remains positive, for given positive values of the density at time t^n, provided that :

$$1 \geq \frac{\Delta t}{2 h_i} \left\{ \frac{S_{i+1/2}}{\widehat{S}_i} \left(s(W_i^n, W_{i+1}^n) + U_i^n \right) + \frac{S_{i-1/2}}{\widehat{S}_i} \left(s(W_{i-1}^n, W_i^n) - U_i^n \right) \right\} \tag{A3}$$

Restricting to a constant cross section profile, the latter condition is the straightforward counterpart of the usual CFL condition :

$$1 \geq \frac{\Delta t}{h} \max_{\{i, i+1\}} \left\{ (|U| + \hat{c})_i, (|U| + \hat{c})_{i+1} \right\}$$

If we turn now to the discrete values of the mass fraction of vapour, we note that :

$$\begin{aligned}\widehat{S}_i h_i (\rho\alpha)_i^{n+1} &= (\rho\alpha)_i^n \left\{ \widehat{S}_i h_i - \frac{\Delta t}{2} \left\{ S_{i+1/2} \left(s(W_i^n, W_{i+1}^n) + U_i^n \right) + S_{i-1/2} \left(s(W_{i-1}^n, W_i^n) - U_i^n \right) \right\} \right\} \\ &+ \frac{\Delta t}{2} \left(s(W_i^n, W_{i+1}^n) - U_{i+1}^n \right) S_{i+1/2} (\rho\alpha)_{i+1}^n + \frac{\Delta t}{2} \left(s(W_{i-1}^n, W_i^n) + U_{i-1}^n \right) S_{i-1/2} (\rho\alpha)_{i-1}^n \end{aligned} \tag{A4}$$

Applying condition (A3), we may conclude that the mean vapour quality α remains positive. Even more, substracting (A1) from (A4), we get :

$$\begin{aligned}\widehat{S}_i h_i (\rho(1-\alpha))_i^{n+1} &= (\rho(1-\alpha))_i^n \left\{ \widehat{S}_i \ h_i - \frac{\Delta t}{2} \left\{ S_{i+1/2} \left(s(W_i^n, W_{i+1}^n) + U_i^n \right) + S_{i-1/2} \left(s(W_{i-1}^n, W_i^n) - U_i^n \right) \right\} \right\} \\ &+ \frac{\Delta t}{2} \left(s(W_i^n, W_{i+1}^n) - U_{i+1}^n \right) S_{i+1/2} (\rho(1-\alpha))_{i+1}^n + \frac{\Delta t}{2} \left(s(W_{i-1}^n, W_i^n) + U_{i-1}^n \right) S_{i-1/2} (\rho(1-\alpha))_{i-1}^n \end{aligned} \tag{A5}$$

Hence, condition (A3) also implies that discrete values of $\rho(1-\alpha)$ remain positive, which completes the proof since discrete values of density are positive.

Appendix B

We focus here on the numerical implementation of subsonic inflow and outflow boundary conditions.

Actually, the same method is applied in both cases, and thus we restrict here on the way to account for imposed pressure in a subsonic outflow. We assume subscript N refers to the last cell on the right of the computational domain and that the fluid flows to the right at the outlet. P_1 is set to be the imposed pressure level in the outlet section, and the unknowns are thus ρ_1, α_1 and U_1 which represent the density , mass fraction of vapour and mean velocity in the outlet section. These are simply determined assuming a 1-rarefaction wave (respectively a one shock wave) connects state « 1 » with state « N » when P_N is greater than P_1 (respectively when $P_N < P_1$). We focus on first case :

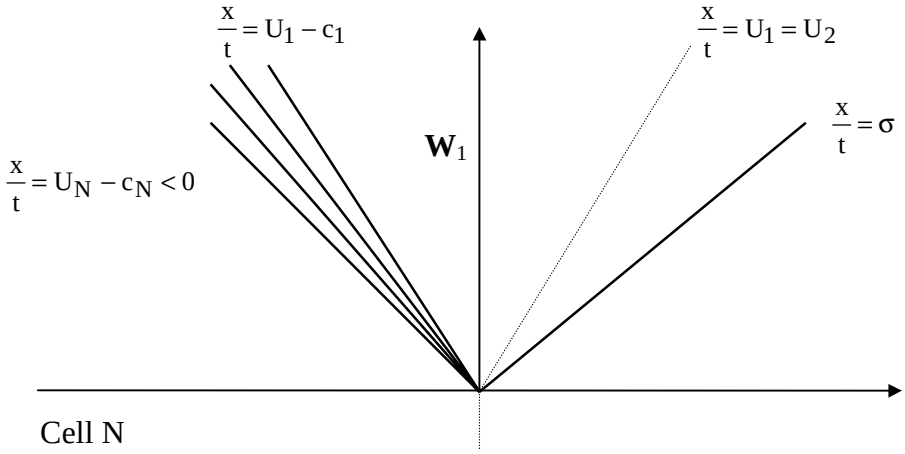

Sketch of wave distribution at the outlet assuming subsonic flow.

Hence , preservation of the 1-Riemann invariants of system gives :

$$\alpha_1 = \alpha_N \tag{B1}$$

$$s(\rho_1, \alpha_1, P_1) = s(\rho_N, \alpha_N, P_N) \tag{B2}$$

$$U_1 = U_N + \int_{\rho_1}^{\rho_N} \frac{c(\rho, \alpha_N, s_N)}{\rho}\, d\rho \tag{B3}$$

Second relation (B2) provides unknown ρ_1 in a straightforward way, since both P_1 and α_1 are given , thanks to (B1). Thus, one may compute the integral on the right side of the last relation, which provides the last unknown U_1. In the opposite case (i.e. when $P_N < P_1$), we use a 1-shock parametrization of curve :

$$\alpha_1 = \alpha_N \tag{B4}$$

$$U_1 = U_N - \left([\rho]_1^N [P]_1^N \left(\rho_1 \rho_N\right)^{-1} \right)^{1/2} \tag{B5}$$

$$[e]_1^N \rho_1 \rho_N = [\rho]_1^N \frac{(P_1 + P_N)}{2} \tag{B6}$$

Obviously, in case of supersonic outflow, no condition should be imposed , and the state at the outlet interface simply is state « N ».

Appendix C

Formulas used to account for mass transfer term are given below.

If : P < 10 bar

$$\theta = 6{,}51\ 10^{-4}\,\alpha^{-0{,}257}\left(\frac{P_S(T_{in}) - P}{P_S(T_{in})}\right)^{-2{,}24}$$

Otherwise

$$\theta = 3{,}84\ 10^{-7}\,\alpha^{-0{,}54}\left(\frac{P_S(T_{in}) - P}{P_C - P_S(T_{in})}\right)^{-1{,}76}$$

In above closures, $P_S(T_{in})$ stands for the saturated pressure corresponding to the inlet temperature and P_C is the thermodynamic critical pressure.

Appendix D

We focus here on VFRoe-ncv scheme with non conservative variable $\mathbf{Y}^t = (\alpha, \tau, U, P)$.

We detail how to get starred value **W(Y*)** . Starting from a uniform section, we rewrite locally at each cell interface the conservative system :

$$\begin{cases} (\rho\alpha)_{,t} + (\rho\alpha U)_{,x} = 0 \\ (\rho)_{,t} + (\rho U)_{,x} = 0 \\ (\rho U)_{,t} + (\rho U^2)_{,x} + P_{,x} = 0 \\ (E)_{,t} + ((E+P)U)_{,x} = 0 \end{cases} \tag{D.1}$$

in a straightforward counterpart (for regular solutions) as follows :

$$\begin{cases} (\alpha)_{,t} + U(\alpha)_{,x} = 0 \\ (\tau)_{,t} + U(\tau)_{,x} - (\tau)(U)_{,x} = 0 \\ (U)_{,t} + U(U)_{,x} + (\tau)P_{,x} = 0 \\ (P)_{,t} + U(P)_{,x} + \hat{\gamma}P(U)_{,x} = 0 \end{cases} \tag{D.2}$$

Hence linearizing around an average state at interface (i+1/2), we get :

$$\mathbf{Y}_{,t} + \mathbf{C}(\mathbf{W}(\mathbf{Y}_i), \mathbf{W}(\mathbf{Y}_{i+1}))\mathbf{Y}_{,x} = 0$$

where :

$$\mathbf{C}(\mathbf{W}(\mathbf{Y}_i), \mathbf{W}(\mathbf{Y}_{i+1})) = \begin{pmatrix} \overline{U} & 0 & 0 & 0 \\ 0 & \overline{U} & -\overline{\tau} & 0 \\ 0 & 0 & \overline{U} & \overline{\tau} \\ 0 & 0 & \overline{\hat{\gamma}}\overline{P} & \overline{U} \end{pmatrix}_{i+1/2}$$

We denote $\mathbf{r}_k$ the basis of right eigenvectors of matrix $\mathbf{C(W(Y_i),W(Y_{i+1}))}$. We introduce the numerical sound velocity at each interface (i+1/2) :

$$\hat{c}^2_{i+1/2} = \overline{\hat{\gamma}}_{i+1/2}\overline{P}_{i+1/2}\overline{\tau}_{i+1/2} \tag{D.3}$$

where :

$$\overline{\phi}_{i+1/2} = \frac{1}{2}(\phi_i + \phi_{i+1}) \tag{D.4}$$

$\mathbf{W}^*_{i+1/2}$ is then given by :

$$\mathbf{W}^*_{i+1/2} = \mathbf{W}(\mathbf{Y}_i) \qquad \text{if } \overline{u}_{i+1/2} - \hat{c}_{i+1/2} > 0$$

$$\mathbf{W}^*_{i+1/2} = \mathbf{W}(\mathbf{Y}_1) \qquad \text{if } \overline{u}_{i+1/2} - \hat{c}_{i+1/2} < 0 \text{ and } \overline{u}_{i+1/2} > 0$$

$$\mathbf{W}^{*}_{\mathbf{i+1/2}} = \mathbf{W}\left(\mathbf{Y_2}\right) \quad \text{if } \bar{u}_{i+1/2} < 0 \text{ and } \bar{u}_{i+1/2} + \hat{c}_{i+1/2} > 0$$

$$\mathbf{W}^{*}_{\mathbf{i+1/2}} = \mathbf{W}\left(\mathbf{Y_{i+1}}\right) \text{ if } \bar{u}_{i+1/2} + \hat{c}_{i+1/2} < 0 \tag{D.5}$$

$\mathbf{Y_1}$ and $\mathbf{Y_2}$ are two intermediate states arising when solving the linear hyperbolic problem :

$$\mathbf{Y_1} = \mathbf{Y_i} + \left(\alpha_1\right)_{i+1/2}\hat{\mathbf{r}}_\mathbf{1} \tag{D.6.a}$$

$$\mathbf{Y_2} = \mathbf{Y_{i+1}} - \left(\alpha_4\right)_{i+1/2}\hat{\mathbf{r}}_\mathbf{4} \tag{D.6.b}$$

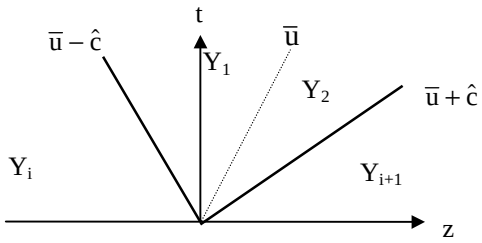

Linearized Riemann Problem

with :

$$\hat{\mathbf{r}}^{t}_{\mathbf{1}} = \left(0, \bar{\tau}_{i+1/2}, \hat{c}_{i+1/2}, -\bar{\hat{\gamma}}_{i+1/2}\ \bar{P}_{i+1/2}\right) \tag{D.7.a}$$

$$\hat{\mathbf{r}}^{t}_{2} = \left(1,0,0,0\right) \tag{D.7.b}$$

$$\hat{\mathbf{r}}^{t}_{3} = \left(0,1,0,0\right) \tag{D.7.c}$$

$$\hat{\mathbf{r}}^{t}_{\mathbf{4}} = \left(0, \bar{\tau}_{i+1/2}, -\hat{c}_{i+1/2}, -\bar{\hat{\gamma}}_{i+1/2}\ \bar{P}_{i+1/2}\right) \tag{D.7.d}$$

Coefficients read :

$$\left(\alpha_1\right)_{i+1/2} = \frac{1}{2}\left[\frac{u_{i+1} - u_i}{\hat{c}_{i+1/2}} - \frac{\bar{\tau}_{i+1/2}}{\hat{c}^2_{i+1/2}}\left(P_{i+1} - P_i\right)\right] \tag{D.8.a}$$

$$\left(\alpha_4\right)_{i+1/2} = -\frac{1}{2}\left[\frac{u_{i+1} - u_i}{\hat{c}_{i+1/2}} + \frac{\bar{\tau}_{i+1/2}}{\hat{c}^2_{i+1/2}}\left(P_{i+1} - P_i\right)\right] \tag{D.8.b}$$

Coefficients are obtained solving :

$$\mathbf{Y}_{i+1} = \mathbf{Y_i} + \sum_{k=1}^{4}\ \left(\alpha_k\right)_{i+1/2}\hat{\mathbf{r}}_k$$

An entropy correction at sonic points in rarefaction waves is required as usual. Owing to the previous decomposition, one may easily see that the numerical intermediate states are in agreement with exact intermediate states since : $P_1 = P_2$, and : $U_1 = U_2$. Moreover, we check that : $\alpha_1 = \alpha_i, \alpha_2 = \alpha_{i+1}$.